Molecular Engineering Strategies for Symmetric Aqueous Organic Redox Flow Batteries

Fornari, Rocco Peter; Mesta, Murat; Hjelm, Johan; Vegge, Tejs; de Silva, Piotr

Published in:
ACS Materials Letters

Link to article, DOI:
10.1021/acsmaterialslett.0c00028

Publication date:
2020

Document Version
Peer reviewed version

Letter

Molecular Engineering Strategies for Symmetric Aqueous Organic Redox Flow Batteries

Rocco Peter Fornari, Murat Mesta, Johan Hjelm, Tejs Vegge, and Piotr de Silva

ACS Materials Lett., **Just Accepted Manuscript** • DOI: 10.1021/acsmaterialslett.0c00028 • Publication Date (Web): 07 Feb 2020

Molecular Engineering Strategies for Symmetric Aqueous Organic Redox Flow Batteries

Rocco Peter Fornari*, Murat Mesta, Johan Hjelm, Tejs Vegge, Piotr de Silva*

Department of Energy Conversion and Storage

Technical University of Denmark

Anker Engelunds Vej 301, 2800 Kongens Lyngby, Denmark

ABSTRACT: Symmetric aqueous organic redox flow batteries (RFBs) are potentially a cheap, durable and safe energy storage technology. Unlike normal asymmetric flow batteries, they are based on electrolytes that exist in at least three oxidation states and can undergo a minimum of two distinct redox processes. We compute the redox potentials of selected electrolytes intending to understand how the interaction between the redox units affects the potentials. We find that electronic interaction between redox units and intramolecular hydrogen bonding can both be exploited to tune the difference between the redox potentials, i.e. the theoretical voltage of the battery. The redox potentials can be further fine-tuned in either direction by adding substituents. Starting from these observations we formulate a set of rules which will help finding ideal candidates for symmetric RFBs.

TOC GRAPHICS

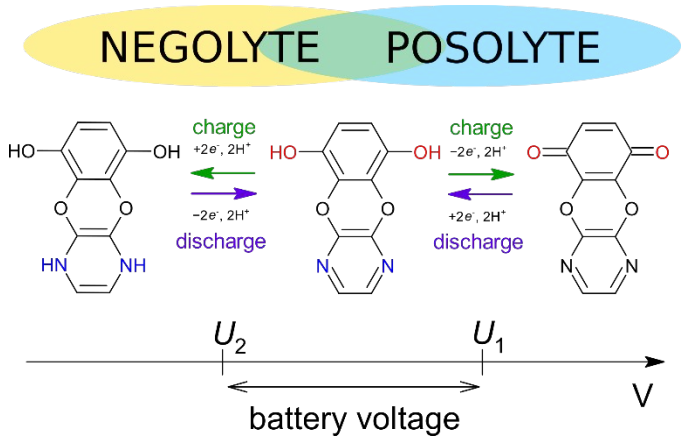

Redox flow batteries (RFB) have the potential to become a long-lasting, low-cost, easily scalable and safe energy storage technology.[1] RFBs based on metal ions are already commercially available but have some drawbacks including highly volatile cost of the active material.[1] Many alternative RFB concepts[2] and active materials[2,3] are currently being developed. All-organic aqueous RFBs, where both active materials are organic molecules, are under intense investigation[4,5] since they hold promise to reduce the cost and the environmental footprint of RFBs. A major challenge for their development is the identification of suitable candidates for the redox-active molecules, which need to have suitable redox potentials, good solubility, long-term chemical stability and low crossover through the separator membrane.[1,6] Computational studies have been used extensively to explore the chemical space of redox-active molecules for RFBs.[7–17] One promising strategy is finding redox molecules which have two redox processes, which could be employed in symmetric RFBs (SRFBs). The main advantage of this concept, as described in details by Potash et al.[18], is that the same species is dissolved in both tanks thereby minimizing the detrimental effects of membrane crossover. Moreover, in the discharged state, the two tanks contain solutions with identical composition, resulting in the absence of any chemical and electrochemical potentials across the cell.[18] A few candidates for aqueous[19–24] and non-aqueous[18,25–31] symmetric RFB electrolytes have

been proposed recently, but no systematic study of structure-property relationships has been reported to date. The common feature of molecules with two redox processes is the presence of (at least) two redox units. If one defines an SRFB as a device with the same composition of the tanks in the discharged state, one could think of a design where two different types of electroactive molecules are dissolved in both tanks. Then, one molecule acts as a posolyte and the other as a negolyte, while half of the material remains inactive. It is not immediately clear whether combining multiple redox units in the same molecule has advantages over such a trivial SRFB. This would be the case if there was a synergy between the redox units either in terms of voltage or solubility. The latter has been explored in combi molecules, where distinct posolyte and anolyte molecules have been covalently connected through solubility-enhancing linkers.[19,21,23] In this contribution, we aim to answer the question whether installing multiple redox moieties on a compact molecular core can lead to additional synergies compared to directly mixing two types of electrolytes or combining them into one molecule through a linker. This is achieved by performing a systematic computational investigation of a class of three-ring candidate molecules for aqueous SRFBs and comparing the results with a judiciously chosen reference system composed of two molecules with just one redox moiety each (vide infra and **Chart S1** in the Supporting

Information). This choice gives us enough flexibility for the exploration of different multi-redox chemistries, while keeping the size of the molecules practically small. The objective of this study is to elucidate new structure-property relationships for bipolar SRFB materials and guide the subsequent experimental molecular design rather than propose a specific new material. Although long-term chemical stability is one of the main challenges in the design of molecules for aqueous RFBs, here we restrict the discussion to electrochemical properties and solubility in water. Our central hypothesis is that the electronic interaction between redox units offers an extra degree of freedom that can be exploited to tune the cell voltage of an SRFB. We will assess the magnitude of this interaction by comparing the potentials of molecules with multiple redox units to those of analogous molecules with a single redox unit.

We build a set of molecules based on an exemplary anthracene-like backbone, a popular template in many state-of-the-art electrolytes.[6,9,10,32,33] We consider a range of prototypical template redox units (1,2-quinone, 1,4-quinone, pyrazine and pyridazine) and build each molecule by introducing two redox units on two of the aromatic rings. Additionally, we consider substitution of two aromatic carbons in the ring without redox-active groups with the oxygen, nitrogen and sulfur heteroatoms. When the heteroatom is nitrogen, this ring becomes a pyrazine, so the molecule effectively

has three redox unit. The molecules with three redox units will be discussed separately. The resulting structures and their indexes are listed in **Chart 1**. On a selected subset of these molecules (see ensuing discussion), we take one step further by adding electron-donating and electron-withdrawing substituents and discuss the impact on redox potentials and solubility.

Chart 1. Structures of the considered electrolytes in their fully oxidized forms.

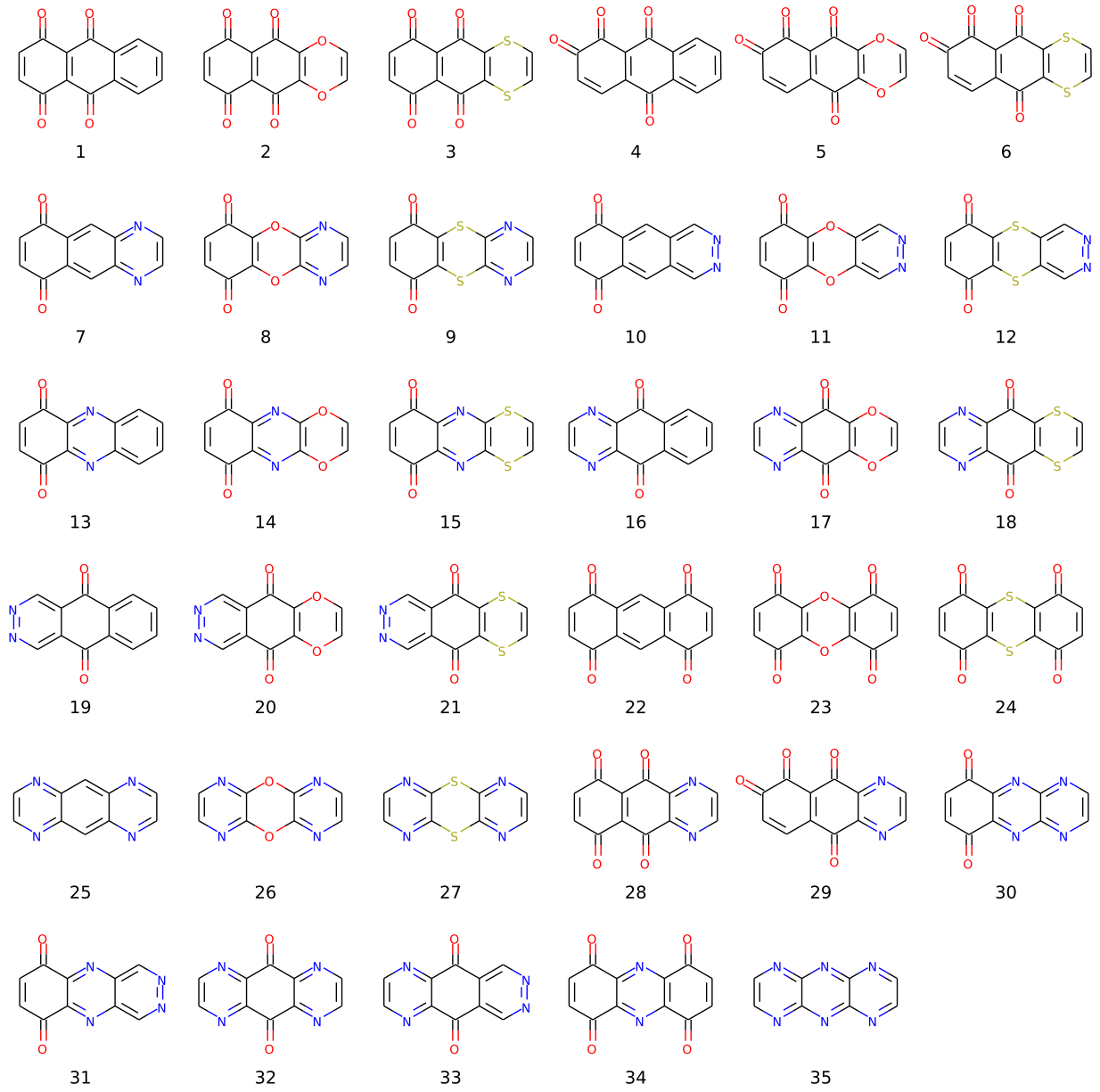

The molecules with two redox units (1-27) are named *double redox* (DR) and can exist in three forms: fully oxidized (A), partially reduced (AH_2) and fully reduced (AH_4). Those with three redox units (28-35) are named *triple redox* (TR) have one further stable state

(AH_6). We assume that all redox processes are concerted two-electron, two-proton reactions, as is the case for most quinone-like species.[6,14,14,22] We evaluate the potentials in water at pH=0, i.e. we consider all species fully protonated to avoid the computation of anions with charge −2, −4 and −6 which can be unreliable with density functional theory (DFT) and implicit solvation models. The redox potentials for the processes $A + 2H^+ + 2e^- \rightarrow AH_2$, $AH_2 + 2H^+ + 2e^- \rightarrow AH_4$ and $AH_4 + 2H^+ + 2e^- \rightarrow AH_6$ are named U_1, U_2 and U_3 respectively, and the difference $\Delta U = U_1 - U_2$ ($\Delta U_{max} = U_1 - U_3$ in TR molecules) is the maximum theoretical voltage of the battery. When the positions of the redox units are not equivalent (molecules 1-21), two different isomers of AH_2 are possible, depending on which redox unit is reduced first. The energy differences between the two isomers are in the range 0.08-2.30 eV for molecules 1-21; when it is small, it should be expected that a mixture of the two isomers can be produced when discharging the battery. For simplicity, we report the potential values determined by the more stable isomer of AH_2, corresponding to the largest possible ΔU. We follow the same approach for the TR molecules (28-35) and choose the most stable of the three isomers of the species AH_2 and AH_4.

For each molecule shown in **Chart 1**, the values of U_1 , U_2 and ΔU are reported in **Figure 1**.

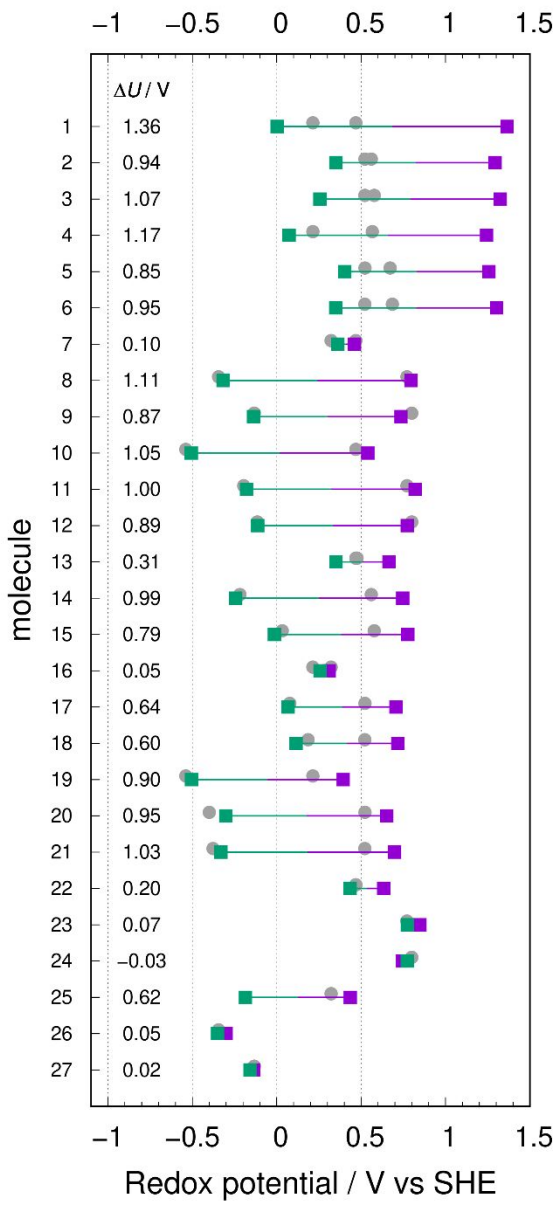

Figure 1. Redox potentials U_1 (purple) and U_2 (green) of molecules 1-27. $\Delta U = U_1 - U_2$ values are listed on the left. The potentials of the single redox (SR) references of each molecule are represented by grey dots.

Some of the considered structures have been already proposed as RFB electrolytes. Derivatives of alizarin and quinizarin

(molecules 1 and 4) have been recently reported to be good candidates for symmetric aqueous batteries;[20,22] the calculated potentials and ΔU of 1 and 4 are consistent with the reported experimental values of alizarin and quinizarin derivatives.[20,22] To understand how ΔU depends on the interaction between the two redox units on a small molecule, we computed for each molecule the redox potentials of two *single redox* (SR) reference molecules, which have only one of the redox units, while the other redox-active ring is just benzenic. For example, the SR references of molecule 8 are shown in **Chart S1** (Supporting Information) and the difference between their redox potentials is ΔU_{SR}. This choice of the reference structures is to a large extent arbitrary as stripping the quinone groups or replacing heteroatoms with carbons not only switches off the redox functionality but also induces global changes in the electronic structure of conjugated rings. Nevertheless, it is the conceptually simplest way to gauge the interactions between multiple redox units on the same molecule. Because the objective of this work is to understand the advantages of merging multiple redox moieties in a single compact molecular core, the choice of reference molecules with the same size of the core is the most natural for such comparisons.

In molecules 1-8, where the redox units are both quinones, ΔU is considerably larger than ΔU_{SR}. This can be interpreted as being due to the electronic interaction between the two non-equivalent

quinone redox units when they are located on the same molecule. In molecule 1, for example, ΔU_{SR} = 0.25 V and ΔU = 1.36 V. However, we note that in molecules 1-8, the increase of ΔU with respect to ΔU_{SR} is predominantly due to U_1 shifting to higher potential rather than U_2 shifting to lower potential. In other words, the reduced species AH_2 and AH_4 are stabilized more than the oxidized species A with respect to the SR references. One reason for this stabilization is the electronic interaction between the (hydro)quinone units, which may be stronger in the more aromatic AH_2 and AH_4 than in the 'quinonic' A. Additionally, we find that a significant component of the stabilization of the reduced species is the intramolecular O–H---O hydrogen bonding; an effect previously reported in literature.[34] To estimate how much of the stabilization is due to hydrogen bonding, we compute for molecule 1 the energies of the conformers of AH_2 and AH_4 with the hydroxyl hydrogens pointing away from the oxygens, i.e. the less stable conformers without hydrogen bonding. As shown in the top panel of **Figure 2**, the stabilization of AH_2 and AH_4 with respect to their less stable conformers is indeed rather large, which results in a +0.3 V shift of U_1 and a +0.4 V increase of ΔU with respect to its conformer without hydrogen bonding (see bottom panel of **Figure 2**). Stabilization of the conformers is likely to be due to a combination of hydrogen bonding and reduced steric repulsion with neighboring hydrogens. A non-negligible conformer stabilization

effect was found to be relevant in a few other molecules, for which comparisons analogous to **Figure 2** are reported in **Figure S4** (Supporting Information).

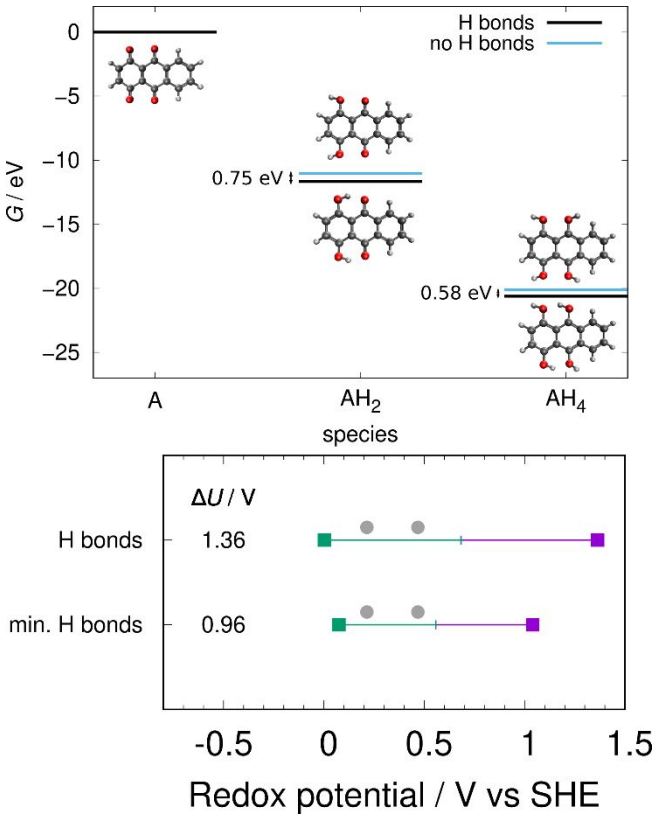

Figure 2. Top: Free energies (relative to the species A) and structures of the solvated reduced forms of molecule 1. Free energies include the thermal correction $G_{\text{gas}}^{\text{corr}}$ and the solvation energy of the protons $n\Delta G_{\text{sol}}(\text{H}^+)$ where n = 4, 2, 0 for (A, AH_2, AH_4). For the reduced species AH_2 and AH_4, the most stable conformer is in black and the conformer with the minimum number of intramolecular hydrogen bonds is in light blue. Bottom: Redox potentials of the conformers shown in the top panel (SR references in gray).

The remaining difference between ΔU_{SR} (gray) and ΔU, without the effect of hydrogen bonds, can be attributed to the electronic interaction between quinones. This effect is observed mainly in molecules where two quinone units are on adjacent rings, where the electronic interaction is stronger and hydrogen bonding between quinone units is possible.

When the two redox units are different (molecules 7-21), the interactions between them appear in general to be weaker. In molecules 7-12, where the redox units are not on adjacent rings, the values of U_1, U_2 and ΔU are very similar to those of their SR references, which in 8-12 already have large ΔU_{SR} values. In molecules 13-15 and 17-21, the significant ~0.2 V positive shift of U_1 with respect to the SR references is due to the electronic interaction between adjacent redox units; additionally, a weak O–H---N hydrogen bond may contribute to the stabilization of AH_2 in molecule 18 (see **Figure S4**, Supporting Information). It is interesting to compare molecules 13 and 16 which are isomers and differ only by the location of the benzene ring: in molecule 16, ΔU = 0.05 V is smaller than ΔU_{SR} = 0.11 V; in contrast, there is a large relative gain in ΔU for molecule 13 (from 0.01 V to 0.31 V). This observation should serve as a warning that the interaction between redox units depends strongly on the electronic structure of the whole molecule and cannot always be guessed from the outset. In general, in the case of multiple redox moieties, the

substituents can strongly interact with all of them, making building intuition harder. Therefore, in such cases accurate calculations of redox potentials should be included in molecular design workflows.

The changes in charge distribution and aromaticity in different redox states for a representative subset of molecules and their associated SR reference structures are shown in **Figure S5** (Supporting Information) in the form of electrostatic potential (ESP) maps and nucleus-independent chemical shifts (NICS) which is a widely accepted measure of aromaticity.[35] Since aromaticity is only one of the components of electronic stabilization energy (which in turn determines the redox potentials), we limit this analysis to qualitative considerations following a recent example.[24] In general, quinone units are non-aromatic and become aromatic when reduced, while pyrazine units are aromatic and become slightly anti-aromatic upon reduction. In molecule 1 the strong interaction between the quinone units is evidenced by the smaller change in aromaticity of the outer redox unit compared to its reference SR_2: when going from A to AH_2, instead of becoming fully aromatic as in SR_2, this hydroquinone shares some electronic density and quinone character with the middle quinone unit. Only when the latter is also reduced to AH_4, the NICS values become more similar to those of the reduced SR references. In molecules 13 and 17 the interaction between the quinone and pyrazine redox units is

evidenced by weaker aromatic and anti-aromatic character in the AH_4 form compared to the SR references. In molecule 8, instead, the oxygen atoms make the middle ring slightly antiaromatic and there is no interaction between the redox units: here the ESP maps and NICS values are very similar to those of the SR reference structures.

In molecules 22-24, the quinone units are not on adjacent units, thereby weakening the interaction and preventing intramolecular hydrogen bonding. The ΔU values are around 0.2 V for the fully aromatic 22 (due to purely electronic interaction) and closer to 0 V for 23 and 24 where the aromaticity is interrupted by the heteroatoms, switching off also the electronic interaction between the redox units. The same pattern is observed in the group 25-27, where the aromatic 25 has large ΔU while in 26 and 27 $\Delta U \sim 0$ V.

We discuss next the redox potentials of molecules 28-35 which have three redox units. The results, shown in **Figure 3**, are consistent with the observations made so far: multiple redox units which are part of the same aromatic system can interact strongly and increase the maximum ΔU. All molecules present a large positive shift of U_1 with respect to the SR reference, which indicates stabilization of the species AH_2 with one of the quinone unit reduced as discussed before. U_3, which is due to the reduction of the pyrazine unit, is always shifted to lower potentials, with the only exceptions being molecules 31 and 33, where it is due to the

pyridazine unit. Overall, the triple redox (TR) design strategy seems another promising way of tweaking the potentials and increasing the theoretical voltage of symmetric RFBs. It should be noted, however, that such a four-state battery, operating between potentials U_1 and U_3, would not be truly symmetric as the tanks would contain different species in the discharged state (AH_2 and AH_4). Such even-state electrolytes may have certain disadvantages for SRFBs as noted by Potash et al.[18] Nevertheless, it has to be noted that this situation is completely analogous to the Vanadium RFB, in which the vanadium ions are oxidized/reduced between the V^{2+}/ V^{3+} and VO^{2+}/VO_2^{+} redox pairs. Despite not being completely symmetric, VRFB enables electrolyte rebalancing strategies that can be used to mitigate the membrane cross-over.

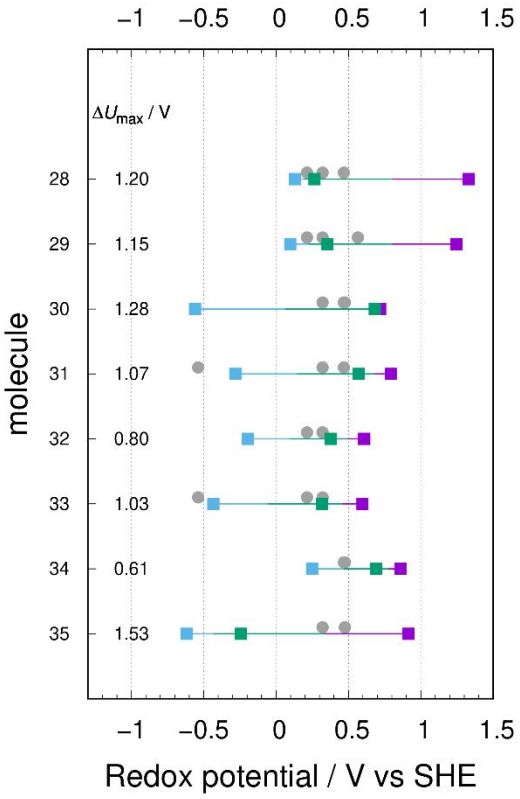

Figure 3. Redox potentials U_1 (purple), U_2 (green) and U_3 (blue) of molecules 28-35. $\Delta U_{max} = U_1 - U_3$ values are listed on the left. The potentials of the single redox (SR) references of each molecule are represented by grey dots.

In summary, we have identified two effects responsible for the increased theoretical voltage of a flow battery based on molecules with multiple redox units compared to the same units on separate molecules: i) electronic interaction between the redox units; ii) intramolecular hydrogen bonding between adjacent units. These effects are strongest in the double quinones 1-6 which can achieve ΔU in the range 0.85-1.36 V compared to ΔU_{SR} of 0.04-0.16 V. When

there are two different redox units, the gain with respect to the SR reference is smaller but can still be of significant magnitude. The interaction between three redox units can also yield significant gains in ΔU.

Another crucial property for RFB electrolytes is the solubility. Although an accurate prediction of solubility is not in the scope of this letter, we are interested how it is affected by the presence of multiple redox units. We report in **Figure 4** the solubilities (predicted with the ChemAxon Solubility Plugin[36]) of molecules 1-35 and of their SR references in the solubility-limiting redox form, which was chosen for each structure as the form with the lowest solubility.

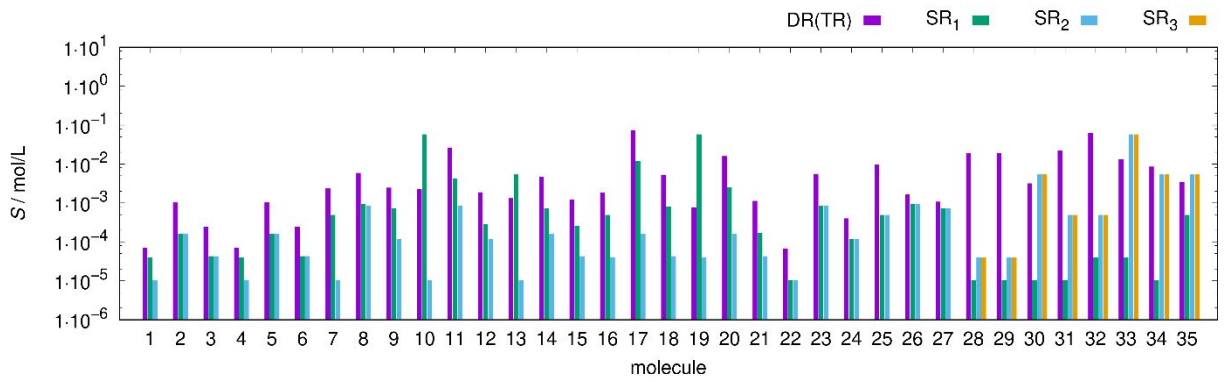

Figure 4. Solubility in water at pH = 0 computed with the ChemAxon Solubility Plugin[36] of double and triple redox molecules (DR, TR) and of their single redox (SR) reference structures. Structures shown in **Chart 1**.

The results show that multiple redox units often improve solubility with respect to molecules of the same size but with a

single redox unit. This should be seen as a positive collateral effect stemming from the proposed design rule of multiple redox units on the same molecular core, whose primary goal is realizing symmetric electrolytes with high potential difference. Once a suitable compound has been found, various strategies can be employed to improve solubility: adding hydrophilic substituents,[4,10] decreasing the melting point by discouraging crystal packing[37] and altering the composition of the electrolyte e.g. by adding chloride salts[38] or exchanging sodium ions with larger hydrophilic organic cations.[20]

We investigate next the effects on the redox potentials of adding electron-donating and electron-withdrawing substituents to a subset of the structures in **Chart 1**. We focus on molecules 1, 8, 31 and 35 because they have large ΔU and are representative of the variety of structures considered. We choose as representative substituents the electron-donating methoxy group (OMe) and the electron-withdrawing sulfonic acid group (SO_3H), whose effects on redox potentials of quinones are roughly the same but with opposite signs.[10] To assess the substituent effect, we consider first single substitution at all available aromatic carbons, then double substitutions at selected positions (see subsequent discussion). The resulting structures are shown in **Chart S2** (Supporting Information). The redox potentials and ΔU of the singly substituted molecules are shown in **Figure S1** (Supporting Information). In

general, OMe tends to shift potentials down and SO_3H tends to shift the potentials up with respect to the unsubstituted molecule, in accordance with previous computational studies on quinones.[10] In particular, we observe that in molecule 8, where the redox units are different and are electronically isolated by the oxygen heteroatoms, the substituent effect is easier to rationalize. OMe has a very small effect when attached to the quinone unit (8a) but shifts U_2 down when attached to the pyrazine unit (8b). SO_3H instead has a greater effect and shifts U_1 up when attached to the quinone unit (8c) and U_2 up when attached to the pyridazine unit (8d). Molecule 1, however, is an exception to this tendency as ΔU becomes smaller with OMe in position 5 and with SO_3H in any position. In the TR molecules (31 and 35), all potentials are in general shifted to lower values. The maximum ΔU is increased in some cases (8b, 8c, 31b, 31c, 35a). In summary, the effect of substituents on the redox potentials is easy to predict when the redox units do not interact strongly.

Since substituents are expected to affect the solubility, we report in **Figure S3** (Supporting Information) the predicted solubilities of the substituted and unsubstituted compounds, each in the solubility-limiting redox form. While in most cases OMe substitution has little effect on solubility, SO_3H mostly yields a significant increase of solubility which is not surprising since it is a hydrophilic group.

With these considerations in mind, one can try to combine one electron-withdrawing and one electron-donating substituent (*push-pull* design strategy) on the same molecule with the goal of increasing ΔU (and therefore the theoretical voltage) while also improving solubility. To this end, we select molecules 8, 31 and 35. In molecules 8 and 31, we add SO_3H to the quinone unit, which we expect to shift U_1 higher, and OMe to the other available redox unit, which should push U_2 lower, thereby obtaining an even larger ΔU. In molecule 35, we adopt the same strategy. We consider both combinations of substitution positions and obtain the molecules 8e, 8f, 31e, 31f, 35c and 35d, as shown in **Chart S2** (Supporting Information). The redox potentials and ΔU of these push-pull doubly substituted molecules are reported in **Figure S2** (Supporting Information). The proposed substitution design strategy proved successful in increasing the ΔU of molecule 8 from 1.11 V (unsubstituted) to 1.23 V (singly substituted with either OMe or SO_3H, 8b or 8c) and 1.33 V (doubly substituted with OMe and SO_3H, 8d and 8f). The predictability of this effect is due to the fact that the two redox units are connected by two oxygen atoms which interrupt the aromatic system and thereby prevent electronic interaction between the redox units. Therefore, the potentials U_1 and U_2 of molecule 8 are individually tunable. In molecules 31 and 35, where the backbone is fully aromatic, the push-pull substitutions did not increase ΔU with respect to single

substitutions. Finally, the double substitution did not significantly affect the solubility compared to single SO_3H substitution (see **Figure S3**, Supporting Information).

Although the goal of this paper is elucidating structure-property relationships and proposing design rules rather than viable candidates for SRFBs, we report in **Tables S1** and **S2** (Supporting Information) the synthetic accessibility (SA) score computed with the RDKit-based implementation[39] of the method described in ref.[40] for all structures considered in all redox forms. A general trend is that molecules with multiple redox units are expected to be more difficult to synthesize than their SR counterparts. Those with more varied heteroatoms are predicted to be less accessible. Among the molecules with ΔU > 0.8 V, those easier to synthetize (with SA score of at least one of the redox forms below 2.6) are 1, 4, 19, 28, 29, 32, 34 and 1a-f, where molecules 1 and 4 have already been synthesized and characterized in an SRFB setup.[20,22]

By computing the redox potentials and solubilities of a representative set of molecules with two and three redox units, we have understood how the interactions between redox units on the same molecule affect the redox potentials and the difference between them. The electronic interaction plays the biggest role in increasing the difference between the redox potentials, and it can be switched off by interrupting the aromatic system between the redox units. Intramolecular hydrogen bonds between redox units on

neighboring rings tend to push the more positive potential to even higher values. The solubility of molecules with multiple redox units is found to be better than their single redox counterparts. Finally, by adding substituents one can fine-tune one or both potentials when the redox units are electronically separated, but substitution effects can be more unpredictable when they are part of the same aromatic system. In this letter we have outlined some fundamental structure-property relationships which enable us to establish guidelines for the design of organic electrolytes for aqueous SRFBs. A complete set of design rules should incorporate tuning of reduction potential, solubility, synthetic accessibility and stability. In this work we primarily have addressed the first, and to some extent the second and third, of these properties. The target for the reduction potential is to achieve as high cell voltage as possible while observing stability limits of the molecule itself and of the aqueous medium in contact with the carbon electrodes and the active materials. In practice this likely limits the cell voltage to < 1.5 V. A symmetric electrolyte with large ΔU and improved solubility can be built in two ways: i) incorporating two or more equivalent redox units on the same aromatic backbone; ii) assembling two or more different redox units which already have a given ΔU_{SR} when on separate molecules. In the latter case, the units can be electronically connected or isolated if the ΔU_{SR} needs to be increased or preserved. The choice of redox

units also determines the absolute positions of the potentials: for example, the double quinone motif is likely to push the more positive potential further up. The potentials may then be tuned further by substitution, keeping in mind the considerations outlined above. The set of design rules outlined here forms a solid basis for future investigations with the goal of finding ideal organic electrolytes for symmetric aqueous redox flow batteries.

COMPUTATIONAL METHODS

All energies are computed at the B3LYP/6-311G(d,p) level of theory with the Q-Chem 5.0 software.[41] The energies in solution are computed with the conductor-like polarizable continuum model (C-PCM)[42–44] using a dielectric constant of 78.39 (water). The reduction potential (in V) for the generic reaction $A + 2H^+ + 2e^- \rightarrow AH_2$ is calculated with the direct approach:[45]

$$U = -\frac{1}{ne}\left(\Delta E_{\mathrm{sol}} + \Delta G_{\mathrm{gas}}^{\mathrm{corr}} + n\Delta G_{\mathrm{sol}}\left(\mathrm{H}^+\right)\right) - U_{\mathrm{SHE}}$$

where $n = 2$ is the number of electrons and protons transferred, e is the elementary charge and the energy differences are expressed in eV. $\Delta E_{\mathrm{sol}} = E_{\mathrm{sol}}(\mathrm{AH_2}) - E_{\mathrm{sol}}(\mathrm{A})$ is the reaction energy computed as the energy difference between the solvated species at the gas phase geometry. $\Delta G_{\mathrm{gas}}^{\mathrm{corr}} = \Delta H_{\mathrm{gas}} - T\Delta S_{\mathrm{gas}}$ is the thermal correction to the reaction free energy (ΔH_{gas} includes zero-point energy and vibrational enthalpy and $-T\Delta S_{\mathrm{gas}}$ is the entropy contribution) computed from vibrational frequency calculations in gas phase at

298 K. The solvation free energy of the proton $\Delta G_{\mathrm{sol}}(\mathrm{H}^+)$ and the standard hydrogen electrode potential U_{SHE} are set to values consistent with the C-PCM solvation model (−11.335 eV and 4.47 V respectively).[46] The solvation free energy is computed as $\Delta G_{\mathrm{sol}} = E_{\mathrm{sol}} - E_{\mathrm{gas}}$ at the gas phase geometry.

ASSOCIATED CONTENT

Supporting Information. Chart explaining the concept of single redox reference structures, structures of molecules with electron-donating and electron-withdrawing substituents, redox potentials and solvation free energies of substituted molecules.

AUTHOR INFORMATION

Corresponding Authors

* E-mail: rocfor@dtu.dk, pdes@dtu.dk

Notes

The authors declare no competing financial interest.

ACKNOWLEDGMENTS

This work was financially supported through an investment by Innovation Fund Denmark via the Grand Solutions project "ORBATS" file nr. 7046-00018B.

REFERENCES

(1) Winsberg, J.; Hagemann, T.; Janoschka, T.; Hager, M. D.; Schubert, U. S. Redox-Flow Batteries: From Metals to Organic Redox-Active Materials. *Angew. Chem. Int. Ed.* **2017**, *56*, 686–711. https://doi.org/10.1002/anie.201604925.

(2) Ding, Y.; Zhang, C.; Zhang, L.; Zhou, Y.; Yu, G. Pathways to Widespread Applications: Development of Redox Flow Batteries Based on New Chemistries. *Chem* **2019**, *5*, 1964–1987. https://doi.org/10.1016/j.chempr.2019.05.010.

(3) Weng, G.-M.; Yang, B.; Liu, C.-Y.; Du, G.-Y.; Li, E. Y.; Lu, Y.-C. Asymmetric Allyl-Activation of Organosulfides for High-Energy Reversible Redox Flow Batteries. *Energy Environ. Sci.* **2019**, *12*, 2244–2252. https://doi.org/10.1039/C9EE00336C.

(4) Leung, P.; Shah, A. A.; Sanz, L.; Flox, C.; Morante, J. R.; Xu, Q.; Mohamed, M. R.; Ponce de León, C.; Walsh, F. C. Recent Developments in Organic Redox Flow Batteries: A Critical Review. *J. Power Sources* **2017**, *360*, 243–283. https://doi.org/10.1016/j.jpowsour.2017.05.057.

(5) Ding, Y.; Zhang, C.; Zhang, L.; Zhou, Y.; Yu, G. Molecular Engineering of Organic Electroactive Materials for Redox Flow Batteries. *Chem. Soc. Rev.* **2018**, *47*, 69–103. https://doi.org/10.1039/C7CS00569E.

(6) Wedege, K.; Dražević, E.; Konya, D.; Bentien, A. Organic Redox Species in Aqueous Flow Batteries: Redox Potentials, Chemical Stability and Solubility. *Sci. Rep.* **2016**, *6*, 39101. https://doi.org/10.1038/srep39101.

(7) Namazian, M.; Coote, M. L. Accurate Calculation of Absolute One-Electron Redox Potentials of Some Para-Quinone Derivatives in Acetonitrile. *J. Phys. Chem. A* **2007**, *111*, 7227–7232. https://doi.org/10.1021/jp0725883.

(8) Zhu, X.-Q.; Wang, C.-H. Accurate Estimation of the One-Electron Reduction Potentials of Various Substituted Quinones in DMSO and CH3CN. *J. Org. Chem.* **2010**, *75*, 5037–5047. https://doi.org/10.1021/jo100735s.

(9) Bachman, J. E.; Curtiss, L. A.; Assary, R. S. Investigation of the Redox Chemistry of Anthraquinone Derivatives Using Density Functional Theory. *J. Phys. Chem. A* **2014**, *118*, 8852–8860. https://doi.org/10.1021/jp5060777.

(10) Er, S.; Suh, C.; Marshak, M. P.; Aspuru-Guzik, A. Computational Design of Molecules for an All-Quinone Redox Flow Battery. *Chem. Sci.* **2015**, *6*, 885–893. https://doi.org/10.1039/C4SC03030C.

(11) Pineda Flores, S. D.; Martin-Noble, G. C.; Phillips, R. L.; Schrier, J. Bio-Inspired Electroactive Organic Molecules for Aqueous Redox Flow Batteries. 1. Thiophenoquinones. *J. Phys. Chem. C* **2015**, *119*, 21800–21809. https://doi.org/10.1021/acs.jpcc.5b05346.

(12) Ding, Y.; Li, Y.; Yu, G. Exploring Bio-Inspired Quinone-Based Organic Redox Flow Batteries: A Combined Experimental and Computational Study. *Chem* **2016**, *1*, 790–801. https://doi.org/10.1016/j.chempr.2016.09.004.

(13) Lin, K.; Gómez-Bombarelli, R.; Beh, E. S.; Tong, L.; Chen, Q.; Valle, A.; Aspuru-Guzik, A.; Aziz, M. J.; Gordon, R. G. A Redox-Flow Battery with an Alloxazine-Based Organic Electrolyte. *Nat. Energy* **2016**, *1*, 1–8. https://doi.org/10.1038/nenergy.2016.102.

(14) Kwabi, D. G.; Lin, K.; Ji, Y.; Kerr, E. F.; Goulet, M.-A.; De Porcellinis, D.; Tabor, D. P.; Pollack, D. A.; Aspuru-Guzik, A.; Gordon, R. G.; et al. Alkaline Quinone Flow Battery with Long Lifetime at PH 12. *Joule* **2018**, *2*, 1894–1906. https://doi.org/10.1016/j.joule.2018.07.005.

(15) Yang, Z.; Tong, L.; Tabor, D. P.; Beh, E. S.; Goulet, M.-A.; De Porcellinis, D.; Aspuru-Guzik, A.; Gordon, R. G.; Aziz, M. J. Alkaline Benzoquinone Aqueous Flow Battery for Large-Scale Storage of Electrical Energy. *Adv. Energy Mater.* **2018**, *8*, 1702056. https://doi.org/10.1002/aenm.201702056.

(16) Tabor, D. P.; Gómez-Bombarelli, R.; Tong, L.; Gordon, R. G.; Aziz, M. J.; Aspuru-Guzik, A. Mapping the Frontiers of Quinone Stability in Aqueous Media: Implications for Organic Aqueous Redox Flow Batteries. *J. Mater. Chem. A* **2019**, *7*, 12833–12841. https://doi.org/10.1039/C9TA03219C.

(17) Goulet, M.-A.; Tong, L.; Pollack, D. A.; Tabor, D. P.; Odom, S. A.; Aspuru-Guzik, A.; Kwan, E. E.; Gordon, R. G.; Aziz, M. J. Extending the Lifetime of Organic Flow Batteries via Redox State Management. *J. Am. Chem. Soc.* **2019**, *141*, 8014–8019. https://doi.org/10.1021/jacs.8b13295.

(18) Potash, R. A.; McKone, J. R.; Conte, S.; Abruña, H. D. On the Benefits of a Symmetric Redox Flow Battery. *J. Electrochem. Soc.* **2016**, *163*, A338–A344. https://doi.org/10.1149/2.0971602jes.

(19) Winsberg, J.; Stolze, C.; Muench, S.; Liedl, F.; Hager, M. D.; Schubert, U. S. TEMPO/Phenazine Combi-Molecule: A Redox-Active Material for Symmetric Aqueous Redox-Flow Batteries. *ACS Energy Lett.* **2016**, *1*, 976–980. https://doi.org/10.1021/acsenergylett.6b00413.

(20) Carretero-González, J.; Castillo-Martínez, E.; Armand, M. Highly Water-Soluble Three-Redox State Organic Dyes as Bifunctional Analytes. *Energy Environ. Sci.* **2016**, *9*, 3521–3530. https://doi.org/10.1039/C6EE01883A.

(21) Janoschka, T.; Friebe, C.; Hager, M. D.; Martin, N.; Schubert, U. S. An Approach Toward Replacing Vanadium: A Single Organic Molecule for the Anode and Cathode of an Aqueous Redox-Flow Battery. *ChemistryOpen* **2017**, *6*, 216–220. https://doi.org/10.1002/open.201600155.

(22) Tong, L.; Jing, Y.; Gordon, R. G.; Aziz, M. J. Symmetric All-Quinone Aqueous Battery. *ACS Appl. Energy Mater.* **2019**, *2*, 4016–4021. https://doi.org/10.1021/acsaem.9b00691.

(23) Zhu, Y.; Yang, F.; Niu, Z.; Wu, H.; He, Y.; Zhu, H.; Ye, J.; Zhao, Y.; Zhang, X. Enhanced Cyclability of Organic Redox Flow Batteries Enabled by an Artificial Bipolar Molecule in Neutral Aqueous Electrolyte. *J. Power Sources* **2019**, *417*, 83–89. https://doi.org/10.1016/j.jpowsour.2019.02.021.

(24) Zhang, C.; Niu, Z.; Peng, S.; Ding, Y.; Zhang, L.; Guo, X.; Zhao, Y.; Yu, G. Phenothiazine-Based Organic Catholyte for High-Capacity and Long-Life Aqueous Redox Flow Batteries. *Adv. Mater.* **2019**, *31*, 1901052. https://doi.org/10.1002/adma.201901052.

(25) Rasmussen, P. G. Electrical Storage Device Utilizing Pyrazine-Based Cyanoazacarbons and Polymers Derived Therefrom. US8080327B1, December 20, 2011.

(26) Oh, S. H.; Lee, C.-W.; Chun, D. H.; Jeon, J.-D.; Shim, J.; Shin, K. H.; Yang, J. H. A Metal-Free and All-Organic Redox Flow Battery with Polythiophene as the Electroactive Species. *J. Mater. Chem. A* **2014**, *2*, 19994–19998. https://doi.org/10.1039/C4TA04730C.

(27) Duan, W.; Vemuri, R. S.; Milshtein, J. D.; Laramie, S.; Dmello, R. D.; Huang, J.; Zhang, L.; Hu, D.; Vijayakumar, M.; Wang, W.; et al. A Symmetric Organic-Based Nonaqueous Redox Flow Battery and Its State of Charge Diagnostics by FTIR. *J. Mater. Chem. A* **2016**, *4*, 5448–5456. https://doi.org/10.1039/C6TA01177B.

(28) Hagemann, T.; Winsberg, J.; Häupler, B.; Janoschka, T.; Gruber, J. J.; Wild, A.; Schubert, U. S. A Bipolar Nitronyl Nitroxide Small Molecule for an All-Organic Symmetric Redox-Flow Battery. *NPG Asia Mater.* **2017**, *9*, e340–e340. https://doi.org/10.1038/am.2016.195.

(29) Ma, T.; Pan, Z.; Miao, L.; Chen, C.; Han, M.; Shang, Z.; Chen, J. Porphyrin-Based Symmetric Redox-Flow Batteries towards Cold-Climate Energy Storage. *Angew. Chem.* **2018**, *130*, 3212–3216. https://doi.org/10.1002/ange.201713423.

(30) Charlton, G. D.; Barbon, S. M.; Gilroy, J. B.; Dyker, C. A. A Bipolar Verdazyl Radical for a Symmetric All-Organic Redox Flow-Type Battery. *J. Energy Chem.* **2019**, *34*, 52–56. https://doi.org/10.1016/j.jechem.2018.09.020.

(31) Hunt, C.; Mattejat, M.; Anderson, C.; Sepunaru, L.; Ménard, G. Symmetric Phthalocyanine Charge Carrier for Dual Redox Flow Battery/Capacitor Applications. *ACS Appl. Energy Mater.* **2019**, *2*, 5391–5396. https://doi.org/10.1021/acsaem.9b01317.

(32) Lin, K.; Chen, Q.; Gerhardt, M. R.; Tong, L.; Kim, S. B.; Eisenach, L.; Valle, A. W.; Hardee, D.; Gordon, R. G.;

Aziz, M. J.; et al. Alkaline Quinone Flow Battery. *Science* **2015**, *349*, 1529–1532. https://doi.org/10.1126/science.aab3033.

(33) Gerhardt, M. R.; Tong, L.; Gómez-Bombarelli, R.; Chen, Q.; Marshak, M. P.; Galvin, C. J.; Aspuru-Guzik, A.; Gordon, R. G.; Aziz, M. J. Anthraquinone Derivatives in Aqueous Flow Batteries. *Adv. Energy Mater.* **2017**, *7*, 1601488. https://doi.org/10.1002/aenm.201601488.

(34) Armendáriz-Vidales, G.; Martínez-González, E.; Cuevas-Fernández, H. J.; Fernández-Campos, D. O.; Burgos-Castillo, R. C.; Frontana, C. The Stabilizing Role of Intramolecular Hydrogen Bonding in Disubstituted Hydroxy-Quinones. *Electrochimica Acta* **2013**, *110*, 628–633. https://doi.org/10.1016/j.electacta.2013.05.123.

(35) Chen, Z.; Wannere, C. S.; Corminboeuf, C.; Puchta, R.; Schleyer, P. von R. Nucleus-Independent Chemical Shifts (NICS) as an Aromaticity Criterion. *Chem. Rev.* **2005**, *105*, 3842–3888. https://doi.org/10.1021/cr030088+.

(36) *Calculator (Version 19.26.0) Developed by ChemAxon, 2019, Https://Chemaxon.Com/Products/Calculators-and-Predictors*; 2019.

(37) Wei, X.; Pan, W.; Duan, W.; Hollas, A.; Yang, Z.; Li, B.; Nie, Z.; Liu, J.; Reed, D.; Wang, W.; et al. Materials and Systems for Organic Redox Flow Batteries: Status and Challenges. *ACS Energy Lett.* **2017**, *2*, 2187–2204. https://doi.org/10.1021/acsenergylett.7b00650.

(38) Milshtein, J. D.; Su, L.; Liou, C.; Badel, A. F.; Brushett, F. R. Voltammetry Study of Quinoxaline in Aqueous Electrolytes. *Electrochimica Acta* **2015**, *180*, 695–704. https://doi.org/10.1016/j.electacta.2015.07.063.

(39) Ertl, P.; Landrum, G. *SAscorer, Https://Github.Com/Rdkit/Rdkit/Blob/Master/Contrib/SA_Score/Sascorer.Py*; 2013.

(40) Ertl, P.; Schuffenhauer, A. Estimation of Synthetic Accessibility Score of Drug-like Molecules Based on Molecular Complexity and Fragment Contributions. *J. Cheminformatics* **2009**, *1*, 8. https://doi.org/10.1186/1758-2946-1-8.

(41) Shao, Y.; Gan, Z.; Epifanovsky, E.; Gilbert, A. T. B.; Wormit, M.; Kussmann, J.; Lange, A. W.; Behn, A.; Deng, J.; Feng, X.; et al. Advances in Molecular Quantum Chemistry Contained in the Q-Chem 4 Program Package. *Mol. Phys.* **2015**, *113*, 184–215. https://doi.org/10.1080/00268976.2014.952696.

(42) Cossi, M.; Rega, N.; Scalmani, G.; Barone, V. Energies, Structures, and Electronic Properties of Molecules in Solution with the C-PCM Solvation Model. *J. Comput. Chem.* **2003**, *24*, 669–681. https://doi.org/10.1002/jcc.10189.

(43) Truong, T. N.; Stefanovich, E. V. A New Method for Incorporating Solvent Effect into the Classical, Ab Initio Molecular Orbital and Density Functional Theory Frameworks for Arbitrary Shape Cavity. *Chem. Phys. Lett.* **1995**, *240*, 253–260. https://doi.org/10.1016/0009-2614(95)00541-B.

(44) Barone, V.; Cossi, M. Quantum Calculation of Molecular Energies and Energy Gradients in Solution by a Conductor Solvent Model. *J. Phys. Chem. A* **1998**, *102*, 1995–2001. https://doi.org/10.1021/jp9716997.

(45) Ho, J. Are Thermodynamic Cycles Necessary for Continuum Solvent Calculation of PKas and Reduction Potentials? *Phys. Chem. Chem. Phys.* **2014**, *17*, 2859–2868. https://doi.org/10.1039/C4CP04538F.

(46) *Organic Electrochemistry*, Fifth edition revised and expanded.; Hammerich, O., Speiser, B., Eds.; CRC Press, Taylor & Francis Group: Boca Raton, 2016.